computed. The results are $L_{e1} = L_{e2} = 19.59$ pH, $L_{e3} = 3.57$ pH and $C_e = -5.83$ fF. The equivalent circuit was then embedded in a transmission line network, Fig. 4(b), including the air-bridge capacitances ($C = 3.5$ fF, calculated using the parallel-plate capacitor approximation) and the lengths of the CPW's from the air-bridges up to the ports defined in Fig. 4(a). Using the MDS software [12], scattering parameters s_{11}, s_{21}, and s_{31} of the network were obtained and compared against those computed by a full-wave electromagnetic simulator [5], Fig. 4(c). For the magnitudes of the scattering parameters, there is excellent agreement between the two methods. The agreement for the phases is good at low frequencies, but deteriorates as frequency increases. The maximum phase error is about 25° at 59 GHz and that has occurred for s_{11}.

The validity of the component values, $L_{e1} = L_{e2} = 54.90$ pH, $L_{e3} = 1.86$ pH, and $C_e = 9$ fF, of the equivalent circuit of a symmetrical T-junction, Fig. 5(a), computed by the present technique was supported experimentally and also confirmed theoretically using the electromagnetic simulator [5], Fig. 5(c). For the measurement, the T-junction had to be shorted at port 1. In this study, the MDS software was used to set up and analyze the equivalent transmission line network of the structure, Fig. 5(b). Some anomalies noted in the experimental results are due to energy leakage into the substrate and resonances and radiation due to long lengths of lines in the structure. In the experiment, the junction was wire-bonded at the reference planes in order to reduce the slot mode effect and as a result, uncertainties arose with the values of the capacitances of these wire-bonds with respect to the center strips. Therefore, these capacitances were not taken into account. However, this should not give rise to a significant error in the results, since the wire-bonds are not close to the metallization and hence should have negligible capacitances. Also, a perfect short circuit was considered for the shorted arm.

IV. Conclusion

A computer technique based on the quasi-static approximation for the determination of the component values of the equivalent circuits of a broad-class of CPW discontinuities was introduced. The technique enjoys the spectral domain formulation in conjunction with the method of moments for approximating the charge distributions at the conductors and the normal component of the magnetic field distribution at the slots. These distributions are used to compute the equivalent capacitances and inductances. The concepts behind the method were illustrated using an example, the CPW T-junction. The convergence of the technique for a T-junction was reported and the equivalent circuit of two other T-junctions were presented. Both the measurements and full-wave electromagnetic simulations supported the accuracy of the results.

References

[1] M. Y. Frankel, S Gupta, J. A. Valdmanis, and G. A. Mourou, "Teraherts attenuation and dispersion characteristics of coplanar lines," *IEEE Trans Microwave Theory Tech.*, vol. 39, pp. 910–915, June 1991.

[2] M. Naghed and I. Wolff, "Equivalent capacitances of coplanar waveguide discontinuities and interdigitated capacitors using a three-dimensional finite difference method," *IEEE Trans. Microwave Theory Tech.*, vol. 38, pp. 1808–1815, Dec. 1990.

[3] M. Naghed, M Rittweger, and I. Wolff, "A new method for the calculation of the equivalent inductances of coplanar waveguide discontinuities," in *IEEE MTT-S Dig.*, 1991, pp. 747–750.

[4] M. Abdo-Tuko, M. Naghed, and I. Wolff, "Novel 18/36 GHz MMIC GaAs FET frequency doublers in CPW-techniques under the consideration of the effects of coplanar discontinuity," *IEEE Trans. Microwave Theory Tech.*, vol. 41, pp. 1307–1315, Aug. 1993.

[5] Sonnet Software Inc., 101 Old Cove Rd., Suite 100, Liverpool, NY 13090.

[6] P. Silvester and P. Benedek, "Equivalent capacitances of microstrip open circuits," *IEEE Trans. Microwave Theory Tech.*, vol. MTT-20, pp. 511–516, Aug. 1972.

[7] A. F. Thomson and A. Gopinath, "Calculation of microstrip discontinuity inductances," *IEEE Trans. Microwave Theory Tech*, vol MTT-23, pp 648–660, Aug. 1975.

[8] M. Riaziat, R. Majidi-Ahy, and I Feng, "Propagation modes and dispersion characteristics of coplanar-waveguides," *IEEE Trans. Microwave Theory Tech*, vol. 38, pp. 245–250, Mar 1990.

[9] W. P. Harokopus and P. B. Katehi, "Radiation loss from open coplanar waveguide discontinuities," in *IEEE MMT-S Dig.*, 1991, pp. 743–746.

[10] D. Mirshekar-Syahkal, *Spectral Domain Method for Microwave Integrated Circuits.* New York: Wiley, 1991.

[11] T. Itoh and A. S. Herbert, "A generalized spectral domain analysis for coupled suspended microstrip lines with tuning septums," *IEEE Trans. Microwave Theory Tech.*, vol. MTT-26, pp. 820–826, Oct. 1978.

[12] Hewlett-Packard Ltd., Cain Rd., Bracknell, Berkshire RG12 1HN, U.K.

High-Power HTS Planar Filters with Novel Back-Side Coupling

Zhi-Yuan Shen, Charles Wilker, Philip Pang, and Charles Carter, III

***Abstract*—Novel back-side coupling was used to produce high-power high temperature superconducting (HTS) filters. Several 2.88 GHz, 0.7% equal-ripple bandwidth, 2-pole TE_{01} mode filters were fabricated using $Tl_2Ba_2CaCu_2O_8$ HTS thin films on 20-mil $LaAlO_3$ substrates. The calibrated, measured performance of the filter at 77 K was <0.1 dB in-band insertion loss and 0.2 dB ripple up to 8 W. The uncalibrated measured performance of the filter was unchanged up to 21 W. This represents a significant advance in the power handling of planar HTS filters. These high-power, high-performance, compact HTS filters were designed to be used in transmitters for satellite communications.**

I. Introduction

High temperature superconducting (HTS) planar filters with excellent microwave performance have been demonstrated at low power [1]. The superior electrical properties of HTS materials are only realized when the current density within the HTS is less than the critical value. The power handling of any HTS filter is thus limited by the peak current and can be improved by either increasing the power handling of HTS materials [2] or by modifying the design to reduce the peak current. Recent progress in increasing the power handling has been made with the use of novel filter structures [3]–[6]. However, if HTS filters are to be used in transmitters, further improvements in power handling will be required. For example, a 1–2% bandwidth multipole filter in a satellite transmitter would be required to handle from 10 W to as much as 100 W. A compact, high-performance HTS filter operating at a temperature of 77 K or above could greatly reduce the size and weight of a transmitter. We report herein a 2.88 GHz, 0.7% equal-ripple bandwidth, two-pole TE_{01} mode HTS planar filter

Manuscript received October 17, 1995; revised February 15, 1996. This work was supported in part by Technology Reinvestment Program NASA Cooperative Agreement NCC 3-344.

The authors are with DuPont, Experimental Station, E304/C114, Wilmington, DE 19880-0304 USA.

Publisher Item Identifier S 0018-9480(96)03782-9.

using novel back-side coupling fabricated using $Tl_2Ba_2CaCu_2O_8$ HTS thin films on a 29 mm×17 mm×0.5 mm $LaAlO_3$ substrate. This filter handled up to 21 W at 77 K with <1% bandwidth and showed no measurable degradation. This represents exceptional performance in a high-power planar filter.

II. Design

The electrical performance characteristics of a filter are determined by both the Q-value of its resonant elements and by its design. HTS thin film materials have a very low surface resistance (R_s) and therefore a very high Q-value which can be used to produce filters with low in-band insertion loss, steep skirts, and high off-band rejection. However, the superior electrical properties of HTS are only realized when the current density everywhere within the film is less than the critical current density (J_c). When the current density at any point exceeds J_c, the R_s increases rapidly causing excessive loss. Therefore, it is not only important to have high quality HTS material but also to make design choices that minimize the local peak current for a given transmitted power.

A filter consists of two basic elements: resonators and coupling circuits. The simplest form for a planar resonator is a half-wavelength rectangular microstrip transmission line. The circulating power within this type of resonator is approximately the loaded Q-value (Q_L) times higher than the transmitted power. Equivalently, the peak current is approximately $\sqrt{Q_L}$ times higher than in a transmission line of the same transverse dimensions. In addition, the current is peaked at the edges due to the local magnetic field concentration. If the peak current at the edge is kept constant, then increasing the width of the resonator would also increase the total current within the resonator. A resonator wider than a square may have transverse modes that significantly complicate the design. Therefore, a two dimensional planar filter structure using square resonators would be a preferred form for HTS filters because of its potential for high-power handling, high Q-value, small size, easy of design, and easy of fabrication. HTS square resonators can also be operated in a dual mode configuration [7]–[8].

The power handling of an HTS filter might also be limited by the input-output coupling circuitry. In most filter designs, a characteristic impedance of 50 Ω for the input and output transmission lines are preferred. A 50 Ω HTS microstrip line on 20-mil $LaAlO_3$ has a width of only 165 μm and can handle only a few watts. Another potential problem involves providing the appropriate coupling strength required by the filter design. There are three commonly used coupling circuits [7]: direct contact, gap coupling, and parallel coupling. A direct coupling circuit usually provides too strong coupling unless some portion of both the input and output lines are very narrow and thus they cannot handle high power. A gap coupling or parallel coupling usually provides too weak a coupling for the input and output circuits unless the gap is very narrow. Narrow gaps can result in very tight fabrication tolerances and rf breakdown.

A novel back-side coupling circuit was used in the design of a two-dimensional planar high-power HTS filter, see Fig. 1. There are two TE_{01} mode square HTS resonators on the front side of the substrate and two coplanar input/output coupling circuits on the back side. The novel back-side coupling has several advantages. The center line width of the coplanar input/output line can be widened to satisfy the power handling but still maintain the desired 50 Ω characteristic impedance. Also, the opening in the ground plane can be adjusted to satisfy the coupling strength with a large coupling gap.

Sonnet Electromagnetic Analysis Software [9] was used to design the filter. The simulation assumed that the filter was driven by a 1 V, 50 Ω source and terminated in a 50 Ω load. A frequency sweep covering the pass-band was used to calculate the S-parameters and

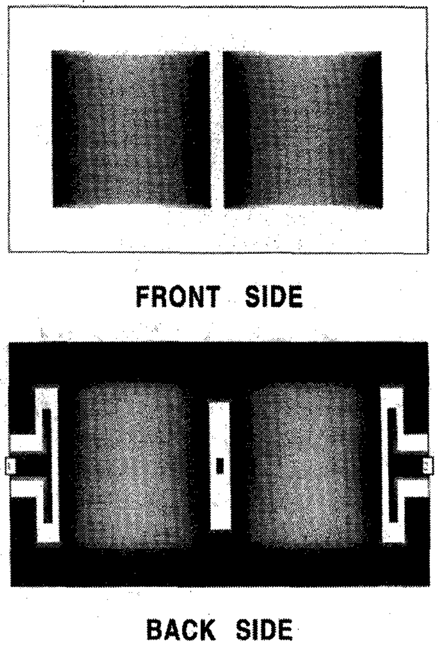

Fig. 1. The circuit layout and the simulated rf current distribution of the two-pole, TE_{01} mode, 2.88 GHz, 0.7% bandwidth HTS filter. The front-side and the back-side patterns are shown in the upper and lower figures. The circuit dimensions are 29 mm × 17 mm. The current density is illustrated by gray shade scale 0 (dark) to 60 (light) A/m at 2.5 mW input power. The bright spots located at the center of the upper and lower edges of the resonators show the peak currents.

the peak current. The maximum current occurs near the equal-ripple frequency points and is located at the center of the upper and lower edges of the resonators, see Fig. 1. The maximum current was used as the criteria to optimize the power handling of the filter design.

III. Fabrication

Two-sided 0.65 μm thick $Tl_2Ba_2CaCu_2O_8$ HTS films deposited on two-inch diameter 20-mil $LaAlO_3$ wafers were used to fabricate the HTS filters [10]. The power handling of $Tl_2Ba_2CaCu_2O_8$ HTS has been reported elsewhere [2]. The HTS wafers were patterned by a standard bi-level photolithography process using ion beam milling. The front-side to back-side alignment was better than 5 μm. Gold contact pads were patterned by a standard lift-off photolithography process. The HTS wafer was diced into individual circuits. The wafer as incorporated into a copper package and was wirebonded with 10-mil gold ribbon. The device was cooled by direct immersion in liquid nitrogen.

IV. Measurement

A specially modified Hewlett-Packard 8720 network analyzer with high power handling option H85 was used for the electrical measurements. The rf signal generated by the network analyzer source was amplified by an external 30 watt Hughes H8020 TWT amplifier. The reference signal was split by an external directional coupler and used by the network analyzer to make the ratioed measurements. The main output of the amplifier was returned to the network analyzer measurement channel. A full two-port calibrated, power-leveled measurement can be performed up to 8 W. The detectors in the network analyzer were protected from the high power by external isolators and internal attenuators.

A full two-port calibration was performed on the network analyzer at room temperature including the cryogenic measurement cables.

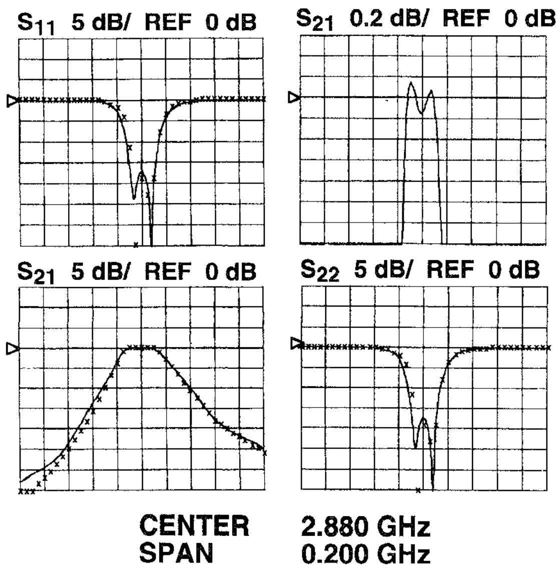

Fig. 2 The calibrated measured S-parameters (—) versus frequency for an HTS filter at 77 K and 8 W input power. A full two-port calibration was performed at room temperature including the cyrogenic measurement cables. When cooled to 77 K, the through insertion loss of the measurement system improved by 0.15 dB. The performance calculated from the numerical simulation assuming $LaAlO_3$ $\epsilon_r = 24$ and liquid nitrogen $\epsilon_r = 1.454$, is shown superimposed (x) on the measured data.

When cooled to 77 K, the insertion loss of the measurement system improved by 0.15 dB. The calibrated S-parameters of the HTS filter were measured at 77 K and 8 W, see Fig. 2. The measured center frequency, 3 dB bandwidth, and equal-ripple bandwidth were 2.88 GHz, 1.40%, and 0.7%, respectively. This compared well with the simulated values of 2.88 GHz, 1.35%, and 0.63%. The measured in-band insertion loss was <0.1 dB with a ripple of 0.2 dB. The two-poles are clearly shown in the S_{11} and S_{22} curves with an in-band return loss of >17 dB. The S_{21} response measured at 8 W was identical to that measured at 0.5 W within the 0.02 dB system error. The S_{21} of the same filter was measured at 77 K from 0.5 W to 21 W, see Fig. 3. When the power was increased to 22 W, the filter response collapsed but recovered when the incident power was reduced. Even though for this measurement the test system can not be calibrated, the very small change of the shape of the S_{21} response up to 21 W shows that the performance does not degrade. By comparison, a similar two-pole HTS filter using the same size square resonators but with a 10 μm front-side coupling gap failed at four watts due to rf breakdown. The damage from the rf breakdown was clearly visible at the edges of the input coupling gap.

V. Summary

A 2.88 GHz, 0.7% bandwidth, two-pole planar HTS filter has been designed and fabricated that can handle up to 21 W of rf power at 77 K with virtually no degradation from its low power performance. To the best of our knowledge, this represents the highest power handling for a planar HTS filter with <1% bandwidth operating at 77 K. The high power handling capability was achieved by a combination of HTS material improvement and novel HTS circuit design. These novel back-side coupling circuits provide adequate coupling strength for the input/output of the HTS filters while avoiding the problems of current crowding, rf breakdown, and tight circuit fabrication tolerances. These coupling circuits can also be used for dual mode or other types of planar HTS filters. This compact HTS filter has demonstrated sufficient power handling for use in transmitters for satellite communications.

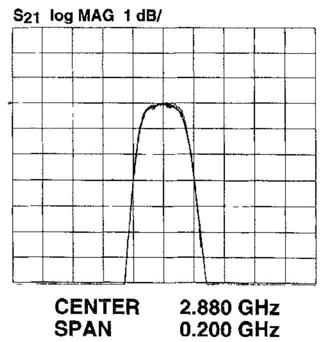

Fig. 3. The uncalibrated S_{21} versus frequency of the HTS filter measured at 77 K and 0.5, 8, 16, and 21 W. The reference level was adjusted at each power level. The 0.2 dB ripple does not show clearly in this figure due to the residual mismatch in an uncalibrated measurement system.

Acknowledgment

The authors would like to thank F. M. Pellicone and R. Cottries for the fabrication of the HTS thin films; S. P. McKenna for the testing the HTS wafers; C. M. Harrington for the patterning and cleaning of the circuits; M. S. Warrington for the fabrication of the gold contact pads; M. S. Brenner for the dicing of the wafer; and C. F. Collier and J. R. Brown for the design of the package.

References

[1] Z.-Y. Shen, *High Temperature Superconducting Microwave Circuits.* Norwood, MA: Artech House, 1994, pp. 112–126.

[2] Z.-Y. Shen and C. Wilker, "Raising the power-handling capability of HTS circuits," *Microwave and RF*, vol. 33-4, pp. 129–138, Apr. 1994.

[3] R. R. Mansour, V. Dokas, S. Ye, F. Thomson, and B. Jolley, "Application of HTS technology to satellite output multiplexers," in *1995 IEEE MTT-S Workshop Sys. Applicat. High Temperature Superconductors and Cryogenic Electrons*, Orlando, FL., May 15, 1995.

[4] G.-C. Liang, D. Zhang, C.-F. Shih, M. E. Johansson, and R. Withers, "High temperature superconducting microstrip filters with high power-handling capability," in *1995 IEEE MTT-S Dig.*, vol. 1, 1995, pp. 191–194.

[5] G -C. Liang, D. Zhang, C.-F. Shih, M. E. Johansson, R. S. Withers, D. E Oates, A. C. Anderson, P. Polakos, P. Mankiewich, E. de Obaldia, and R E. Miller, "High-power HTS microstrip filters for wireless communication," *IEEE Microwave Theory Tech.*, vol. 43, pp. 3020–3029, 1995

[6] A. Enokihara, K Mizuno, and K. Setsune, "High-Tc superconducting planar filter for power handling capability," in *Int. Superconductive Electron Conf.*, Nagaya, Japan, Sept. 18–21, 1995.

[7] J A. Curtis and S. J. Fiedziuszko, "Dual mode microstrip filters," *Appl. Microwave Mag.*, pp. 86–93, Fall 1991.

[8] ——, "Miniature dual mode microstrip filters," in *1991 IEEE MTT-S Dig.*, vol. 2, 1991, pp. 443–446.

[9] J. C. Rautio and R. F. Harrington, "An electromagnetic time-harmonic analysis of shielded microstrip circuits," *IEEE Microwave Theory Tech.*, vol. MTT-35, pp. 726–730, 1987.

[10] W. L. Holstein, L. A. Parasi, Z.-Y. Shen, C. Wilker, M. S. Brenner, and J. S. Martens, "Surface resistance of large-area $Tl_2Ba_2CaCu_2O_8$ thin films at microwave and millimeter wave frequencies measured by three noncavity techniques," *J. Supercond.*, vol 6, pp. 191–200, 1993.